

Vibrational Spectra in Spinel-Type Mixed Systems

$\text{Cd}_x\text{Zn}_{1-x}\text{Cr}_2\text{Se}_{4(1-y)}\text{S}_{4y}$

KUNIO WAKAMURA

*Department of Natural Science, Okayama University of Science,
1-1 Ridai-cho, Okayama-city, Okayama 700, Japan*

Received December 1, 1986; in revised form July 20, 1988

Infrared transmission spectra were measured for three kinds of mixed systems, $\text{Cd}_x\text{Zn}_{1-x}\text{Cr}_2\text{Se}_{4(1-y)}\text{S}_{4y}$ ($x = 1$, $y = 1$, and $x = y = 0.2$), from 50 to 900 cm^{-1} at 300 and 16 K. Based on the experimental data, observed vibrational modes are assigned to three one-mode and one two-mode behaviors among four T_{1u} optical modes of $\text{Cd}_x\text{Zn}_{1-x}\text{Cr}_2\text{S}_4$ and two one-mode and two two-mode behaviors for $\text{CdCr}_2\text{Se}_{4(1-y)}\text{S}_{4y}$. From the squared frequency difference for the longitudinal and transverse optical modes, $\omega_{LO}^2 - \omega_{TO}^2$, a dominant contribution of ionic character of vibrational mode to the mode behavior is suggested for several spinel-type mixed systems. In the more disordered mixed system, $x = y = 0.2$, five bands were observed and their characteristics are discussed. © 1989 Academic Press, Inc.

Introduction

The vibrational modes of mixed systems have been classified into two types, named one-mode and two-mode behaviors (1, 2). One-mode behavior exhibits only one band for all compositions and shows continuous energy variation from one end member to another end member. Phonon damping shows relatively small increase at intermediate composition x . A two-mode behavior exhibits two main bands at x and their frequencies vary slightly with x . For the intensity and the damping constant, both bands exhibit opposite composition dependence from each other.

The mixed system $AB_{1-x}C_x$ exhibits only one of the two-mode behaviors. On the contrary, the spinel-type mixed system exhibits both kinds of mode behaviors among the four infrared active modes. For mixed-cation systems, $M_x\text{Zn}_{1-x}\text{Cr}_2\text{S}_4$ ($M = \text{Cd}, \text{Hg}$)

and $\text{Hg}_x\text{Zn}_{1-x}\text{Cr}_2\text{Se}_4$, the three higher energy modes show one-mode behaviors and the lowest energy modes show two-mode behaviors (3-5). A mixed system $\text{Cd}_x\text{Zn}_{1-x}\text{Cr}_2\text{Se}_4$, which is described here with the notation $\langle x, 0 \rangle$, shows only one-mode behavior (6). On the other hand, anion mixed systems, $M\text{Cr}_2\text{Se}_{4(1-y)}\text{S}_{4y}$ ($= \langle 1, y \rangle$) for $M = \text{Cd}$ and $\langle 0, y \rangle$ for $M = \text{Zn}$) show complex phonon spectra and those mode behaviors have not been assigned clearly (7, 8).

This variety in types of mode behavior may also depend on the site occupied by the substituted atom, that is A-, B-, or X-site in a spinel AB_2X_4 . This effect would appear remarkable in a more complicated mixed system, such as $\text{Cd}_x\text{Zn}_{1-x}\text{Cr}_2\text{Se}_{4(1-y)}\text{S}_{4y}$, because plural substituted atoms at the cation and anion sites may induce the multiple effect. However, such investigation of spinels has not been performed.

In this paper, we measured the composition dependencies of infrared absorption spectra for the mixed systems, $\langle x, 1 \rangle$, $\langle 1, y \rangle$, and a more disordered mixed crystal $\langle 0.2, 0.2 \rangle$. In the spinels, powdered crystals have been mainly utilized for the analysis of phonon spectra since a large single crystal cannot be easily grown (9). For more reliable analysis, the transmission spectra should be compared with those of the single crystal or the reflection spectra. Such comparison was attempted for HgCr_2Se_4 (10) and CdIn_2S_4 (11) and both spectra showed reasonable agreement. In this paper, a spectrum of $\langle x, 1 \rangle$ is compared with its reflection spectrum. For the assignment of mode behavior in the mixed systems $\langle 1, y \rangle$ and $\langle x, 1 \rangle$, two parameters, namely, differences of phonon frequency and of the bandwidth of the phonon mode at both end members, are introduced. The classification of mode behavior for many other spinel-type mixed systems is also examined using these parameters. The results verify the tentative analysis of observed results.

Experiments

Powdered crystals of $\langle x, 1 \rangle$ were prepared by heating stoichiometric amounts of ZnCr_2S_4 and CdCr_2S_4 at 820°C in an evacuated quartz tube for 10 days. The mixed system $\langle 1, y \rangle$ was prepared with a similar procedure at 780°C . The more disordered mixed crystal system $\langle 0.2, 0.2 \rangle$ was prepared from the mixed crystals of $\langle 0.2, 1 \rangle$ and $\langle 0.2, 0 \rangle$ by heating them at 760°C for a few months. Since their X-ray diffraction patterns showed only the peaks predicted from the end members, it was concluded that they possessed the spinel structure. The samples were annealed until better crystallization was accomplished, which was judged from the half-width of X-ray diffraction pattern at high angle region. The composition x and y for $\langle x, 1 \rangle$ and $\langle 1, y \rangle$ were determined from Vegard's law (6).

For determining the composition of $\langle 0.2, 0.2 \rangle$, Vegard's law was also assumed. Values determined almost equal the compositions deduced from the elements before the reaction.

For measuring the transmission spectra, several samples were prepared. That is, 6, 15, and 40 mg of powder crystals were dispersed in 250 mg polyethylene at 140°C , and were compacted into disks 2 mm thick and 150 mm^2 in area. To make uniform the dependency of powder size on the spectra, the powder was ground below 200 mesh. The spectra were measured from 50 to 900 cm^{-1} by using a Fourier transform spectrometer (Digilab Inc., FTS-20E) at 300 and 16 K. The resolution is 1.0 cm^{-1} . For the low-temperature measurements, a cell equipped with a closed solvey cycle system was set at the spectrometer evacuated to 10^{-6} Torr. The temperature at the sample holder was measured with a constantan-Au (0.07%Fe) thermocouple.

Results and Analysis

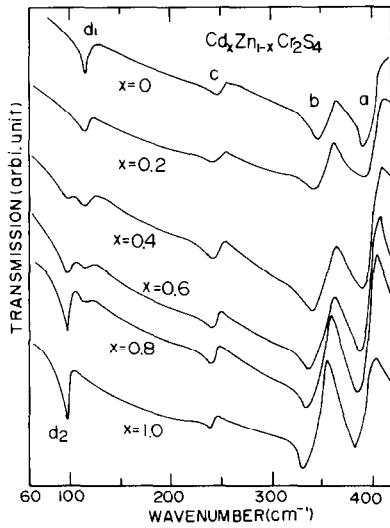
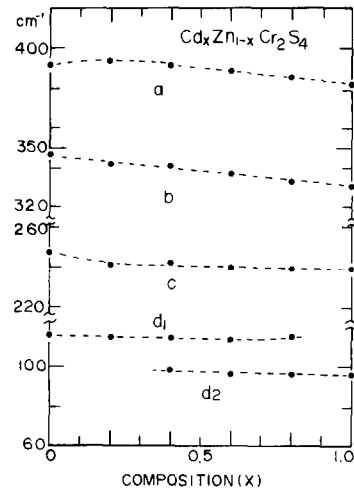
In a normal spinel AB_2X_4 , the phonon modes at the Γ point are represented as

$$\Gamma_{\text{vib}} = A_{1g} + E_g + 2A_{2u} + 2E_u + T_{1g} + 3T_{2g} + 5T_{1u} + 2T_{2u},$$

where $4T_{1u}$ represents the four infrared active optical modes and A_{1g} , E_g , and $3T_{2g}$ are Raman active modes. The composition dependencies of $4T_{1u}$ modes are described in the following sections.

1. $\text{Cd}_x\text{Zn}_{1-x}\text{Cr}_2\text{S}_4$

The transmission spectra for $\langle x, 1 \rangle$ are shown in Fig. 1. Five bands a , b , c , d_1 , and d_2 were observed at intermediate compositions. We observed clear structure for the d_1 -band even at $x = 0.8$, though it was not observed in the reflectivity spectra (3). This fact suggests that the transmission spectra may be more sensitive to a weak absorption


 FIG. 1. Transmission spectra for $(x, 1)$.

 FIG. 2. Composition dependence of peak frequency ω_0 for $(x, 1)$. Dashed lines represent smooth curves through the experimental points.

than the reflectivity spectra. The frequencies obtained for the four absorption peaks ($= \omega_0$) at $x = 0$ and $x = 1$ are very near that of the transverse mode ($= \omega_{\text{TO}}$) in each end member (12). These are assigned to the four infrared active modes predicted from the crystal symmetry. Their composition dependencies are shown in Fig. 2 and also listed in Table I. From the characteristics mentioned in the first section and also from the small frequency difference between

both end members, the a -, b -, and c -bands obey one-mode behavior. On the other hand, the d -bands obey two-mode behavior because of the characteristic composition dependencies of the d_1 - and d_2 -bands. This assignment agrees with the results already reported (3). The absorption intensities of d_1 - and d_2 -bands also seem to vary consistently with x , which may bear a meaning for the nearly equal frequencies of those bands. Since the effect of multiple scatter-

TABLE I

x, y	$\text{Cd}_x\text{Zn}_{1-x}\text{Cr}_2\text{S}_4$					$\text{CdCr}_2\text{Se}_{4(1-y)}\text{S}_{4y}$					$\text{Cd}_x\text{Zn}_{1-x}\text{Cr}_2\text{Se}_{4(0.8)}\text{S}_{4(0.2)}$					
	a	b	c	d_1	d_2	a_1	a_2	b_1	b_2	c	d	a_2	b_1	b_2	c	d
0	392	347	247	116	—	288	—	271	—	188	76	360	285	307	206	92
0.2	396	342	241	115	—	—	346	272	294	186	76	354	279	304	195	91
0.4	391	341	242	115	98	—	355	274	301	191	78	—	—	—	—	—
0.6	389	336	240	115	97	—	366	—	315	206	83	—	—	—	—	—
0.8	385	333	239	115	96	—	377	—	323	232	92	—	—	—	—	—
1.0	382	330	238	—	96	—	382	—	330	239	96	346	272	294	186	76

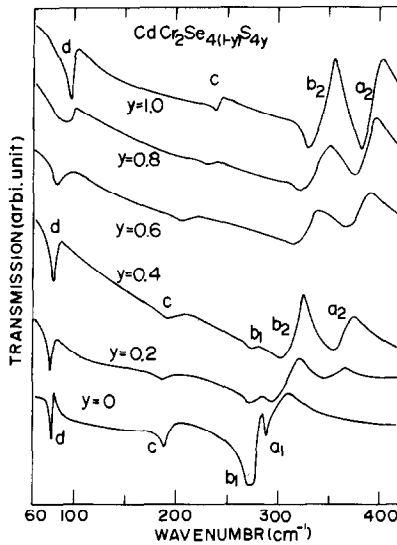


FIG. 3. Transmission spectra for $\langle 1, y \rangle$.

ing on the spectra depends on particle size in the sample and the wavelength of incident light, it will appear nearly equally in the spectra of both bands. The reasonable variation of absorption intensity observed for the phonon bands in the mixed system $\text{Hg}_x\text{Zn}_{1-x}\text{Cr}_2\text{Se}_4$ may also confirm this assumption (5).

2. $\text{CdCr}_2\text{Se}_4(1-y)\text{S}_4y$

Transmission spectra for the mixed system $\langle 1, y \rangle$ are shown in Fig. 3. Four bands a_1 , b_1 , c , and d were observed for $y = 0$ and also the bands a_2 , b_2 , c , and d were observed for $y = 1$. Since the magnitudes of ω_0 for these bands are nearly equal to those of ω_{TO} reported already (4, 8, 12), those bands are also assigned to the four infrared active modes predicted from the crystal symmetry.

Five bands a_2 , b_1 , b_2 , c , and d were observed at intermediate composition y . The magnitudes of ω_0 are shown as a function of y in Fig. 4 and listed in Table I. For the c - and d -bands, only one band was observed over all compositions. Its frequency varies

continuously with y . Therefore, they obey one-mode behavior. On the other hand, the other two modes obey two-mode behavior since we can attribute the a_2 - and b_2 -bands at $y \neq 1$ to the a_2 - and b_2 -bands at $y = 1$ and also the b_1 -band at $y \neq 0$ to the b_1 -band at $y = 0$. This assignment characterizes the feature of typical two-mode behavior. However, we cannot observe the band which should be attributed to the a_1 -band at $y = 0$. This result may be caused by the accidental closing together of the a_1 - and b_2 -bands at x . From Reileigh's theorem, the b_2 -band at x does not take a higher energy than that of a_1 -band (13). If the frequency shift of the a_1 -band with x is proportional to that of the a_2 -band and the frequency of the a_1 -band is almost equal to that of the b_2 -band, only one band will be observed, as seen in Fig. 3. A similar feature was observed for the mixed systems of $\langle 0, y \rangle$ (4, 7). This suggestion will be supported from the magnitudes of parameters mentioned later.

To confirm the above assignment, we measured the infrared absorption spectra

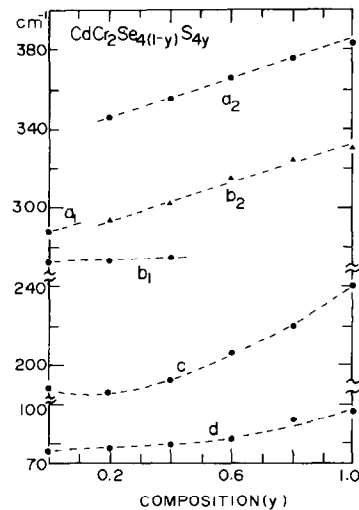


FIG. 4. Composition dependence of peak frequency ω_0 for $\langle 1, y \rangle$. Dashed lines represent smooth curves through the experimental points.

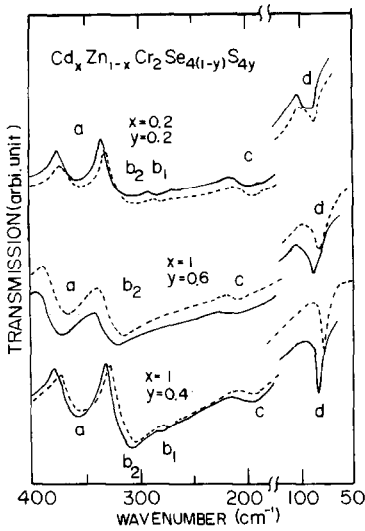


FIG. 5. Transmission spectra at 16 and 300 K. Solid and dashed lines show those at 16 and 300 K, respectively.

for $\langle 1, 0.4 \rangle$ and $\langle 1, 0.6 \rangle$ at low temperature. The spectra are shown in Fig. 5. Although the frequencies of the observed bands at 16 K shift several wavenumbers from those at 300 K to the higher frequency side, the peak corresponding to the a_1 -band was not observed.

3. $\text{Cd}_x\text{Zn}_{1-x}\text{Cr}_2\text{Se}_4(1-y)\text{S}_4y$

The spectra for the mixed systems of $\langle 0, 0.2 \rangle$, $\langle 0.2, 0.2 \rangle$, and $\langle 1, 0.2 \rangle$ are shown in Fig. 6. The values ω_0 for those are shown as a function of x by the curves through the experimental points in Fig. 7. The shift of ω_0 with x is small for the observed five bands and characterizes one-mode behavior. However, the broadening of b_2 - and c -bands in $\langle 0.2, 0.2 \rangle$ is considerably large in comparison with that of the one-mode-type phonon band in normal mixed crystals. To check the origin of this broadening, the values of $(\omega_{LO} + \omega_{TO})/2$ for the four end members are plotted by the vertical lines in Fig. 6. These correspond to the frequencies of absorption peaks at the end members.

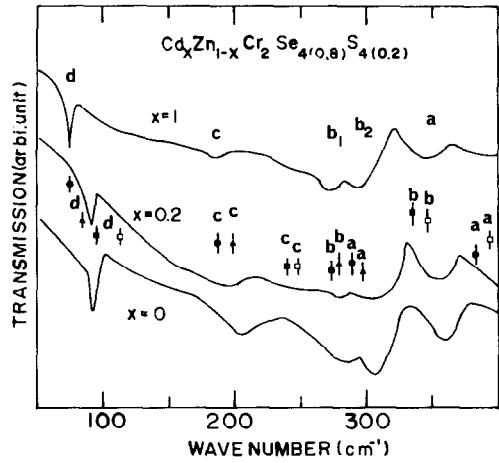


FIG. 6. Transmission spectra for the mixed crystals $\langle 1, 0.2 \rangle$, $\langle 0, 0.2 \rangle$, and $\langle 0.2, 0.2 \rangle$. The vertical lines indicate the positions of phonon frequencies in each end member. For the end members, $\langle 1, 0 \rangle$, $\langle 1, 1 \rangle$, $\langle 0, 1 \rangle$, and $\langle 0, 0 \rangle$ are shown by the closed circles, closed and open squares, and closed triangles, respectively.

Since they take the value within limited narrow frequency range, overlapping of those bands can produce the broadbands at x , though the frequency of those shift with x .

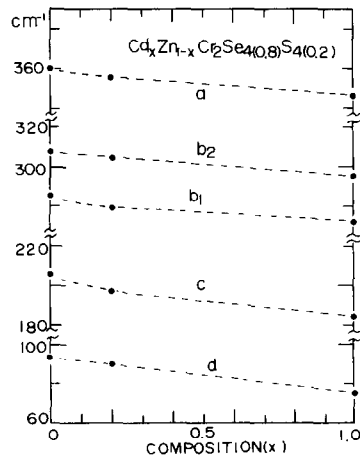


FIG. 7. Composition dependence of peak frequency ω_0 for $\langle x, 0.2 \rangle$. Dashed lines indicate smooth curves through the experimental points.

To test this prediction, the spectrum of $\langle 0.2, 0.2 \rangle$ at 16 K was measured and is shown in Fig. 5. Although the maximum of the five observed bands exhibit small shifts to higher frequencies, sharpening of the band at low temperature was not clearly observed. However, the considerable broadening of d -band, observed at 16 K in $\langle 0.2, 0.2 \rangle$, may relate to the overlapping of bands.

Discussion

For the classification of mode behavior in pseudo-binary alloy, it has been pointed out that the atomic mass, force constant, and effective charge are important parameters (1, 2, 14). In the spinels, such classification is not easy because several modes in a mixed system exhibit the different types of mode behaviors. Each parameter mentioned above contributes to each mode with different magnitudes. To clarify the role of each parameter, its effect on the mode behavior must be separately investigated. In this section, we discuss the effect of ionicity upon the bands and explain the mode behaviors for the mixed systems $\langle 1, y \rangle$, $\langle 0, y \rangle$, and $\langle 0.2, 0.2 \rangle$. Some physical values characterizing the mode behaviors are also discussed.

Onodera and Toyozawa (15) proposed a mode criterion for the behavior of exciton bands in pseudo-binary alloy. This criterion employs the frequency difference and the difference of bandwidth for the end members. By analogy to this criterion, we employ the ratio T/Δ , in which $\Delta [= (\omega_{LO} - \omega_{TO})_{x=1} + (\omega_{LO} - \omega_{TO})_{x=0}]$ and $T [= \omega_{TO}(x=1) - \omega_{TO}(x=0)]$ are introduced using data for the end members. Values of T/Δ , T/ω_s , and $r (= |A_1 - A_s|/A_s)$ are listed in Table II together with values of ω_{LO} and ω_{TO} , where ω_s stands for the smaller value of ω_{TO} at $x=0$ and $x=1$. The notation A_s or A_1 indicates a small or large magnitude of $A (= \omega_{LO}^2 - \omega_{TO}^2)$ at the end members. The value T and

r represent the frequency difference between both end members and the difference of ionicity between the end members, respectively.

In the table, we find two characteristic features. The first is that the d -mode requires a considerably large magnitude of T/ω_s in comparison with the other three modes a , b , and c . The second is that a large magnitude of r is found for the more ionic modes a and b in $\langle 0, y \rangle$ and $\langle 1, y \rangle$, which show two-mode behavior despite the small magnitude of T/ω_s . The critical value of r which classifies the mode behaviors into one-mode or two-mode type seems empirically to be between 0.7 and 0.8. Small r shows one-mode type and roughly means the empirical relationship proposed for pseudo-binary alloys (1, 2); that is, if the energy of the reststrahlen band at the end members overlap, the one-mode behavior will appear. The value of T/Δ is not always a good parameter for classifying the mode behaviors.

From these results, we suggest that the ionicity is important for classifying the behavior of more ionic modes. For less ionic modes, the influence of frequency difference between the end members, which is described by T/ω_s , is rather dominant; that is, the observed two-mode behaviors in Table II are found for $T/\omega_s > 0.4$ and also one-mode behavior for $T/\omega_s < 0.4$. All Raman active modes in $\text{Cd}(\text{In}_{1-x}\text{Cr}_x)_2\text{S}_4$, therefore, are predicted to be one-mode type and agree with the assignment reported already (16). The only exception is found for d -mode in $\langle x, 1 \rangle$. For d -mode, value of the force constant is important as pointed out by Wakamura *et al.* (5). This result exhibits that the frequency and the force constant provide different roles on mode behavior. It is perhaps a character of multinary compounds because the phonon frequency is determined from the combination of several force constants. The classification of modes predicted from the values r and T/ω_s are

TABLE II
 ω_{TO} AND ω_{LO} FOR THE END MEMBERS IN THE 10 MIXED SYSTEMS

Compound	Mode	Frequencies (cm^{-1})				Parameters			Mode assignment	
		$x = 0, y = 0$		$x = 1, y = 1$		r	T/ω_s	T/Δ	Obs.	Predic.
		ω_{TO}	ω_{LO}	ω_{TO}	ω_{LO}					
$\text{CdCr}_2\text{Se}_{4(1-y)}\text{S}_{4y}$	a	287.0	292.0	378.0	391.0	2.45	0.32	5.1	2	2
	b	264.0	281.0	321.5	350.0	1.07	0.22	1.3	2	2
	c	187.0	189.0	239.0	241.0	0.28	0.29	13.6	1	1
	d	74.0	76.0	95.0	97.5	0.60	0.28	4.6	1	1
$\text{ZnCr}_2\text{Se}_{4(1-y)}\text{S}_{4y}$	a	296.0	300.5	387.0	403.0	3.71	0.31	4.5	2	2
	b	272.5	289.0	336.0	361.5	0.92	0.23	1.5	2	2
	c	199.0	201.0	247.0	249.5	0.55	0.24	10.6	1	1
	d	85.5	87.5	114.5	116.5	0.34	0.36	7.7	1	1
$\text{Zn}_{1-x}\text{Cd}_x\text{Cr}_2\text{S}_4$	a	387.0	403.0	378.0	391.0	0.26	0.02	0.3	1	1
	b	336.0	361.5	321.5	350.0	0.08	0.04	0.2	1	1
	c	247.0	249.5	239.0	241.0	0.29	0.03	1.6	1	1
	d	114.5	116.5	95.0	97.5	0.04	0.20	4.2	2	1
$\text{Zn}_{1-x}\text{Cd}_x\text{Cr}_2\text{Se}_4$	a	296.0	300.5	287.0	292.0	0.08	0.03	0.9	1	1
	b	272.5	289.0	264.0	281.0	0.0	0.03	0.2	1	1
	c	199.0	201.0	187.0	189.0	0.06	0.06	2.8	1	1
	d	85.5	87.5	74.0	76.0	0.15	0.16	3.0	1	1
$\text{Zn}_{1-x}\text{Hg}_x\text{Cr}_2\text{Se}_4$	a	296.0	300.5	285.0	290.0	0.07	0.04	1.2	1	1
	b	272.5	289.0	270.0	281.0	0.53	0.01	0.1	1	1
	c	199.0	201.0	170.0	172.0	0.17	0.17	7.2	1	1
	d	85.5	87.5	57.5	60.0	0.18	0.49	6.3	2	2
$\text{Zn}_{1-x}\text{Hg}_x\text{Cr}_2\text{S}_4$	a	387.0	403.0	373.0	384.5	0.45	0.04	0.5	1	1
	b	336.0	361.5	327.0	350.5	0.12	0.03	0.2	1	1
	c	247.0	249.5	228.0	231.0	0.11	0.08	3.3	1	1
	d	114.5	116.5	69.5	74.5	0.56	0.65	6.4	2	2
$\text{Cd}_{1-x}\text{Hg}_x\text{Cr}_2\text{Se}_4$	a	287.0	292.0	285.0	290.0	0.01	0.01	0.2	—	1
	b	264.0	281.0	270.0	281.0	0.53	0.02	0.2	—	1
	c	187.0	189.0	170.0	172.0	0.10	0.10	4.2	—	1
	d	74.0	76.0	57.5	60.0	0.02	0.29	3.7	—	1
$\text{Cd}(\text{In}_{1-x}\text{Cr}_x)_2\text{S}_4$	a	307.0	339.0	378.0	391.0	1.07	0.23	1.6	—	2
	b	215.0	270.0	321.5	350.0	0.39	0.50	1.3	—	2
	c	171.0	172.0	239.0	241.0	1.80	0.40	22.7	—	2
	d	68.0	69.0	95.0	97.5	2.51	0.40	7.7	—	2
$\text{Cd}_{1-x}\text{Hg}_x\text{Cr}_2\text{S}_4$	a	378.0	391.0	373.0	384.5	0.15	0.01	0.2	—	1
	b	321.5	350.0	327.0	350.5	0.30	0.02	0.1	—	1
	c	239.0	241.0	228.0	231.0	0.43	0.05	2.2	—	1
	d	95.0	97.5	69.5	74.5	0.50	0.37	3.4	—	1
$\text{HgCr}_2\text{Se}_{4(1-y)}\text{S}_{4y}$	a	285.0	290.0	373.0	384.5	2.03	0.31	5.3	—	2
	b	270.0	281.0	327.0	350.5	1.63	0.21	1.7	—	2
	c	170.0	172.0	228.0	231.0	1.01	0.34	11.6	—	2
	d	57.5	60.0	69.5	74.5	1.45	0.21	1.6	—	2

Note. The number 1 or 2 in the last column indicates one-mode or two-mode type predicted from r and T/ω_s .

listed in the last column in Table II for the 10 mixed systems.

The important role of ionicity on phonon modes in spinels was already suggested in the lattice dynamical model proposed for pure spinels by Lauwers and Herman (17). The model contains the short-range force constants and the effective charge. It gives better agreement for the observed frequencies than that by Brüesch and Ambrogio (18) which contains only the short-range valence forces.

We can also understand the origin of broadbands in $\langle 0.2, 0.2 \rangle$ (Fig. 6) from the difference of ionicity. Following the model proposed by Wakamura *et al.* (5), many kinds of structural units are considered in $\langle x, y \rangle$. Each unit requires different magnitudes for the force constant and the effective charge. Therefore, the phonon characterized by each unit has a different frequency. For more ionic modes, the effective charge or the force constant in each unit contributes, with slight difference, to the phonons since the dominant Coulomb force smooths the difference of the value in each unit because of its long-range interaction. Hence, the phonon frequencies characterized by each unit will be close together and produce a broadband. Such a broadband was observed for one-mode-type phonon in a more ionic alloy $K_{0.5}Rb_{0.5}Cl_{0.5}Br_{0.5}$ (19). On the other hand, the low ionic modes are affected differently from the force constant or the effective charges in each unit. Such modes have been observed in semiconducting alloys, $Ga_{1-x}Al_xAs_{1-y}P_y$ (20), $(GaP)_x(InAs)_{1-x}$ (21, 22), $TlGa_xIn_{1-x}Se_{2x}S_{2(1-x)}$ (23), etc. In the first alloy, the frequencies of observed bands are nearly equal to those for their four end members and the characteristic properties of phonon modes for the end members, GaAs, GaP, AlAs, and AlP, were observed. A similar feature may also be observed in other mixed systems. These results support the explanation mentioned above.

Acknowledgment

We thank Professor S. Minomura of Okayama University of Science for helpful discussions and for the critical reading of the manuscript.

References

1. I. F. CHAND AND S. S. MITRA, *Adv. Phys.* **85**, 359 (1971).
2. A. S. BARKER, JR. AND A. J. SIEVERSE, *Rev. Mod. Phys.* **47**(Suppl. 2), S140 (1975).
3. K. WAKAMURA, H. IWATANI, AND K. TAKARABE, *J. Phys. Chem. Solids* **48**, 857 (1987).
4. H. D. LUTZ AND H. HAEUSELER, *J. Solid State Chem.* **13**, 215 (1975).
5. K. WAKAMURA, T. ARAI, S. ONARI, K. KUDO, AND T. TAKAHASHI, *J. Phys. Soc. Japan* **35**, 1430 (1973).
6. K. WAKAMURA, T. ARAI, AND K. KUDO, *J. Phys. Soc. Japan* **40**, 1118 (1976).
7. V. E. RIEDEL AND E. HOVATH, *Z. Anorg. Allg. Chem.* **371**, 248 (1969).
8. H. D. LUTZ AND M. FEHER, *Spectrochim. Acta A* **27**, 357 (1971).
9. S. I. BOLDISH AND W. B. WHITE, *J. Solid State Chem.* **25**, 121 (1978).
10. K. WAKAMURA, S. ONARI, T. ARAI, AND K. KUDO, *J. Phys. Soc. Japan* **31**, 1845 (1971); T. H. LEE, T. COBURN, AND R. GLUCK, *Solid State Commun.* **9**, 1821 (1971).
11. K. YAMAMOTO, T. MURAKAWA, Y. OHBAYASHI, H. SHIMIZU, AND K. ABE, *J. Phys. Soc. Japan* **35**, 1258 (1973).
12. K. WAKAMURA, T. OGAWA, AND T. ARAI, *Japan. J. Appl. Phys.* **19** (Suppl. 19), 249 (1980).
13. A. A. MARADUDIN, E. W. MONTROLL, AND G. H. WEISS, "Theory of Lattice Dynamics in the Harmonic Approximation," Academic Press, New York (1963).
14. K. WAKAMURA AND T. ARAI, *J. Appl. Phys.* **62**, 1750 (1987).
15. Y. ONODERA AND Y. TOYOZAWA, *J. Phys. Soc. Japan* **24**, 341 (1968).
16. J. WATANABE, M. UDAGAWA, T. KAMIGAICHI, AND K. OHBAYASHI, *J. Phys. C* **19**, 2351 (1986).
17. H. A. LAUWERS AND M. A. HERMAN, *J. Phys. Chem. Solids* **41**, 223 (1980).
18. P. BRÜESCH AND F. D. AMBROGIO, *Phys. Status Solidi B* **50**, 514 (1972).
19. J. F. ANGRESS, W. G. CHAMBERS, G. A. GLEDHILL, AND W. SMITH, *J. Phys. C* **19**, 3717 (1976).

20. P. N. SEN AND G. LUCOVSKY, *Phys. Rev. B* **12**, 2998 (1975).
21. N. N. SIROTA, I. V. BONDNAR, AND G. F. SMIRNOVA, *Phys. Status Solidi A* **41**, 669 (1977).
22. G. M. ZINGER, M. A. IL'IN, E. P. RASHEVSKAYA, AND A. I. RYSKIN, *Sov. Phys. Solid State* **21**, 1522 (1979).
23. K. R. ALLAKHVERDIEV, M. M. GODZHAEV, A. I. NADZHAFOV, AND R. M. SARDARLY, *Sov. Phys. Solid State* **24**, 1442 (1982).